Multifunctional HER2-Antibody Conjugated Polymeric Nanocarrier-Based Drug Delivery System for Multi-Drug-Resistant Breast Cancer Therapy

Raju Vivek,*[†,⊥] Ramar Thangam,[†,‡,⊥] Varukattu NipunBabu,[†] Chandrababu Rejeeth,[†] Srinivasan Sivasubramanian,[‡] Palani Gunasekaran,[‡] Krishnasamy Muthuchelian,[∥] and Soundarapandian Kannan*[†,§]

[†]Proteomics & Molecular Cell Physiology Laboratory, Department of Zoology, School of Life Sciences, Bharathiar University, Coimbatore 641 046, Tamilnadu, India

[‡]Department of Virology, King Institute of Preventive Medicine & Research, Guindy, Chennai 600 032, Tamilnadu, India

[§]Department of Zoology, Periyar University, Salem 636 011, Tamilnadu, India

[∥]Department of Bioenergy, School of Energy, Environment & Natural Resources, Madurai Kamaraj University, Madurai 625 021, Tamilnadu, India

S Supporting Information

ABSTRACT: Nanotechnology-based medical approaches have made tremendous potential for enhancing the treatment efficacy with minimal doses of chemotherapeutic drugs against cancer. In this study, using tamoxifen (Tam), biodegradable antibody conjugated polymeric nanoparticles (NPs) was developed to achieve targeted delivery as well as sustained release of the drug against breast cancer cells. Poly(D,L-lactic-co-glycolic acid) (PLGA) NPs were stabilized by coating with poly(vinyl alcohol) (PVA), and copolymer polyvinyl-pyrrolidone (PVP) was used to conjugate herceptin (antibody) with PLGA NPs for promoting the site-specific intracellular delivery of Tam against HER2 receptor overexpressed breast cancer (MCF-7) cells. The Tam-loaded PVP−PLGA NPs and herceptin-conjugated Tam-loaded PVP−PLGA NPs were characterized in terms of morphology, size, surface charge, and structural chemistry by dynamic light scattering (DLS), Transmission electron microscopy (TEM), ζ potential analysis, ^{1}H nuclear magnetic resonance (NMR), and Fourier transform infrared (FT-IR) spectroscopy. pH-based drug release property and the anticancer activity (in vitro and in vivo models) of the herceptin conjugated polymeric NPs were evaluated by flow cytometry and confocal image analysis. Besides, the extent of cellular uptake of drug via HER2 receptor-mediated endocytosis by herceptin-conjugated Tam-loaded PVP−PLGA NPs was examined. Furthermore, the possible signaling pathway of apoptotic induction in MCF-7 cells was explored by Western blotting, and it was demonstrated that drug-loaded PLGA NPs were capable of inducing apoptosis in a caspase-dependent manner. Hence, this nanocarrier drug delivery system (DDS) not only actively targets a multidrug-resistance (MDR) associated phenotype (HER2 receptor overexpression) but also improves therapeutic efficiency by enhancing the cancer cell targeted delivery and sustained release of therapeutic agents.

KEYWORDS: biodegradable polymers, antibody conjugated nanocarrier, tamoxifen, drug delivery systems (DDS), multidrug resistance (MDR), breast cancer therapy
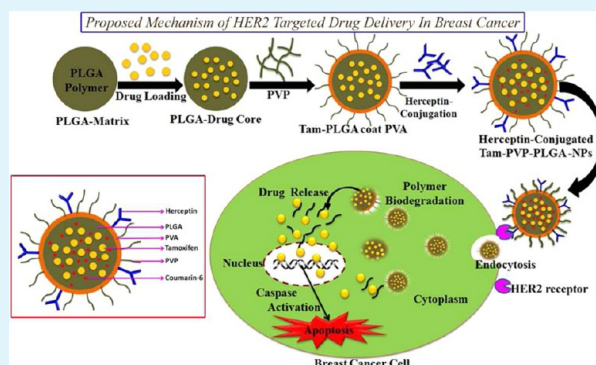

INTRODUCTION

Chemotherapy is a predominant treatment strategy against cancer wherein anticancer drugs are used to induce cell death in cancer cells. However, it has several limitations such as the requirement of high drug dose, adverse effects, non specificity, targeted drug delivery, gradual development of drug resistance, and multidrug resistance (MDR) that reduce the efficacy of the therapy.[1,2] Though nanotechnology based therapeutic approaches are promising for multimodality treatment, their potential is high especially in enhancing the delivery of anticancer drug to tumor tissue with minimizing its distribution and toxicity in healthy tissue.,[1,3−9] To overcome the limitations associated with chemotherapy, nanomedicine strategies employing the formulations of anticancer drugs in various nanocarrier forms have been reported.[6−9]

Scheme 1. Schematic Illustration of the Fabrication Process for PLGA Nanoparticles Incorporated with Tamoxifen Drug[a]
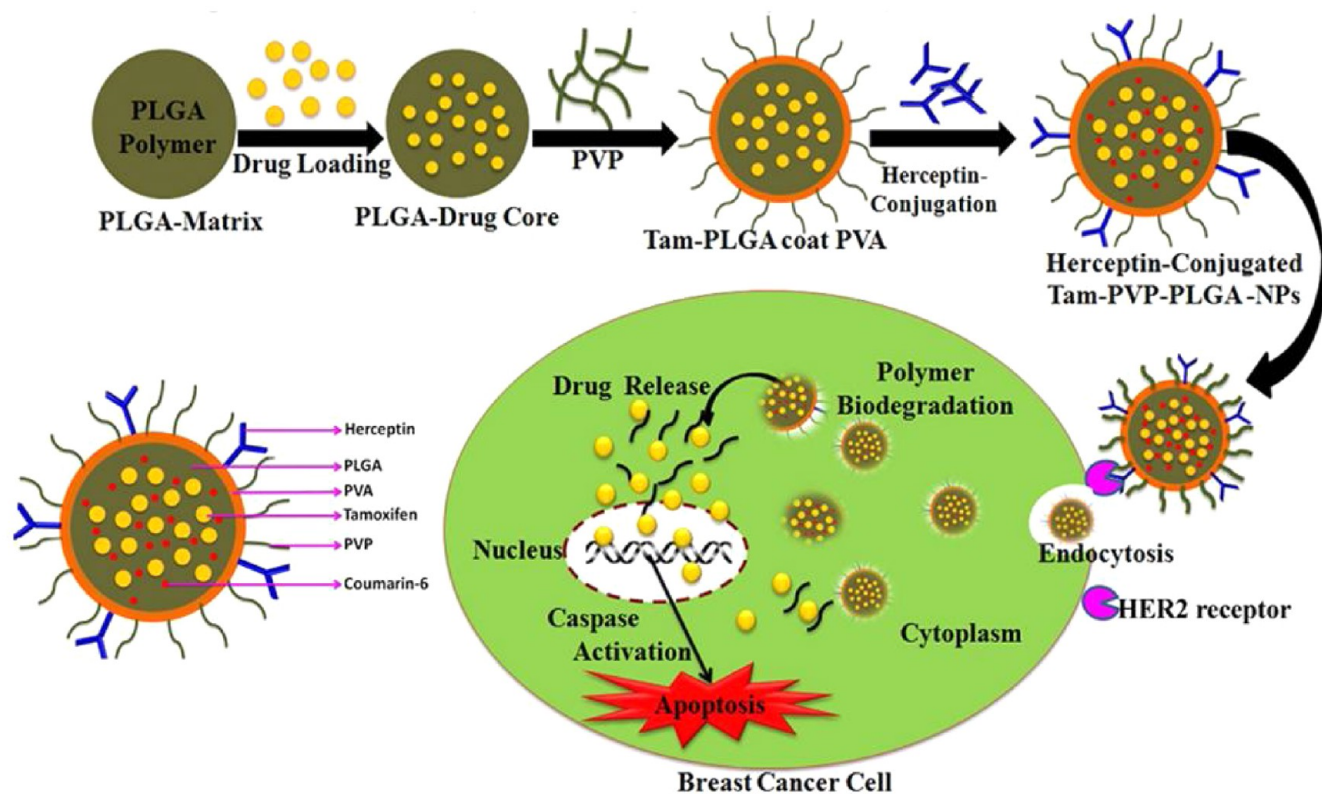
[a]Therapeutic mechanism of herceptin−Tam−PVP−PLGA NPs could specifically enter into breast cancer cells via HER2 receptor mediated endocytosis process; under acidic conditions which degraded PLGA led to releases of Tam from the nanoparticles then released Tam entered inside the MCF-7 cells and activated caspase enzyme followed by induction of apoptosis.

Breast cancer is a globally prevalent cancer having high incidence and mortality rates.[10,11] Chemotherapeutic drugs are effective in the form of mono or combination therapy for treating breast cancer. Tamoxifen (Tam) belongs to a class of non steroidal triphenylethylene derivatives, and is the first selective estrogen receptor modulator.[12−14] Herceptin has been widely used for treating breast cancer due to overexpression of human epidermal growth factor receptor-2 (HER2) by cells.[10,13,15] Combination of Tam with herceptin promotes the therapeutic efficacy in treating HER2 positive metastatic breast cancers. The role of HER2 in the pathogenesis of breast cancer has been well reported.[10] Among the various antigens present on HER2 overexpressed breast cancer cells, the biomarker HER2 has been used for targeted drug delivery.

Polyvinyl-pyrrolidone (PVP), a polymer approved by U.S. Food and Drug Administration (U.S. FDA), has potential skin penetration properties, and its clinical utility as blood plasma expander is well reported.[16,17] PVP may be preferred to polyethelene glycol (PEG) for preparation methods involving freeze-drying because of its lyo and cryoprotectant properties. Furthermore, PVP is shown to interact with a variety of hydrophilic and hydrophobic pharmaceutical agents and enhances the solubility of micelles.[18−20] PLGA NPs are much preferred controlled release polymer systems because of their clinical safety. They have also emerged as drug carriers in novel drug delivery systems due to its hydrophobic nature, which aids effective entrapment of hydrophobic drugs into PLGA NPs.[21−23] PLGA has carboxylic groups that enable conjugation of the targeting residues, and it enhances cytosolic delivery of NPs following endocytosis.[24] These polymer conjugates can be passively accumulated in the targeted tumors.[25,26] A number of polymer-anticancer drug conjugates have been tested in clinical trials for their effectiveness in targeted delivery and cellular uptake of drugs.[27]

In the present study, we have developed a novel polymeric nanocarrier platform of Herceptin-conjugated Tamoxifen drug delivery system (DDS) based on PVP−PLGA NPs designated for HER2 targeted delivery. In the NP formulation process, PVA coating was performed to increase the colloidal stability, and PVP was used as a surfactant. Herceptin was then conjugated on the surface of NP for achieving targeted drug delivery, as well as therapeutic action against HER2-over-expressing cancer cells. Characterization of Tam-loaded PVP−PLGA NPs (Tam−PVP−PLGA NPs) and herceptin-conjugated Tam-loaded PVP−PLGA NPs (herceptin−Tam−PVP−PLGA NPs) in terms of particle size measurement and its distribution, and particle surface features such as morphology, charge and structural chemistry was performed by methods such as DLS, TEM, ζ potential analysis, ^{1}H NMR and FT-IR spectroscopy. Encapsulation efficiency (EE) and in vitro release kinetics of the drug were studied. Cellular uptake of PVP−PLGA NPs with or without herceptin-conjugation in vitro was quantitatively measured by ELISA plate reader and examined by confocal laser scanning microscopy. Therapeutic efficiency of the herceptin−Tam−PVP−PLGA NPs was evaluated in vitro by performing studies on MCF-7 cell toxicity and apoptosis and compared with that of the Tam−PVP−PLGA NPs formulation. The process involved in the fabrication of PLGA nanoparticles incorporated with Tam drug, can be used to conjugate with Herceptin antibody, when the

nanoparticles targeted the breast cancer cells, the nanoparticles enter into the cytoplasm by HER2 receptor mediated endocytosis effects. Tamoxifen is then released from nanoparticles at low pH which degrades polymer and resulting in inhibition of tumor cell growth through apoptosis (Scheme 1).

■ EXPERIMENTAL SECTION

Materials. Poly(D,L-lactic-co-glycolic acid) (PLGA) (lactic acid/glycolic acid = 50:50), poly(N-vinylpyrrolidone) (PVP) (MW = 10 000), poly(vinyl alcohol) (PVA), coumarin-6 (fluorescence marker), and 3-(4, 5-dimethylthiazol-2-yl)-2,5-diphenyltetrazolium bromide (MTT) were sourced from Hi-Media, India. Tamoxifen (Tam), 4′,6-diamidino-2-phenylindole (DAPI), fluorescent isothiocynate (FITC), propidium iodide (PI), dimethyl sulfoxide, EDC (1-ethyl-3-(3-(dimethylamino)propyl)-carbodiimide), Bradford reagent, and other analytical grade chemicals were obtained from Sigma-Aldrich, India. All the samples were prepared using deionized water (dH$_2$O). The human breast cancer cell line (MCF-7) was purchased from National Centre for Cell Sciences (NCCS), Pune, India and it was maintained in Dulbecco's Modified Eagle's Medium (DMEM) supplemented with 10% fetal bovine serum (FBS, GIBCO, U.S.A.) and 1% antibiotic-antimycotic solution. Cells were grown to confluence at 37 °C in 5% CO$_2$ atmosphere. A fixed number of cells were seeded into cell culture (96, 24, and 6 wells) plates (Nunc, USA) and maintained for further studies. Animal experiments were performed using female BALB/c nude mice of 6 weeks old after obtaining prior approval of the Institutional Animal Ethical Committee, adhering to the guidelines of Committee for the Purpose of Control and Supervision of Experiments on Animals constituted by the Animal Welfare Division of India.

Preparation of Tam−PVP−PLGA NPs. Tam-loaded PLGA NPs were prepared by w/o/w double emulsion-solvent evaporation method. Briefly, 20 mg of Tam was dissolved in 0.3 mL of dH$_2$O and poured into 3 mL of PVP (5 mg/mL) solution containing 150 mg of PLGA dispersed in chloroform (w/o), followed by sonication in an ice bath using a Sonicator (Sonics, CT, U.S.A.) for 30 s at 50% amplitude with an energy output of 500 W. An aliquot (100 mL) of ammonium bicarbonate solution (90 mg/mL) was then added to the mixture and sonicated again for 30 s. The primary emulsion obtained was emulsified in 25 mL ice-cold 0.1 M sodium chloride solution (pH 7.0) containing 0.5% (w/v) of poly(ethyl methacrylate) (PEMA) for 2 min at 4000 rpm using a laboratory Mixer. For obtaining double emulsion, the primary emulsion was added drop wise with 2 mL of 5% (w/v) PVA solution and sonicated again for 90 s. The double emulsion was then added to 20 mL of 0.3% (v/v) PVA solution and stirred overnight at 500 rpm. The resultant emulsion was added to 50 mL of dH$_2$O and evaporated at 40 °C for 5 h with gentle stirring. To conjugate the antibody with the prepared Tam−PVP-PLGA NPs, 1 mg of HER (Herceptin®, Roche Pharma Ltd.) was dissolved in 400 mL of PBS and mixed with 100 mL of the prepared nanoparticle solution (10 mg mL^{-1}). The NPs were harvested by centrifugation process, washed thrice with dH$_2$O and lyophilized. Coumarin-6 loaded NPs were prepared by the above said method through mixing 5 μL of 1 mg/mL coumarin-6 solution with 0.95 mL of solvent containing 20 mg of the polymer.

Conjugation of Herceptin with PLGA NPs. EDC reagent was used to facilitate the conjugation of herceptin onto the NP surface as reported by Kocbek et al.[40] with slight modifications. Briefly, 5 μg of EDC was added to 360 μL mixture having 400 μg of NPs and 400 μg of herceptin, and the reaction mixture was mixed gently for 2 h at room temperature (RT). The molar ratio of EDC to herceptin was ∼8.8. The immuno-nanoparticles were dispersed in 100 μL of PBS and the protein content was determined by Bradford assay. Two controls such as one lacked EDC and the other lacked both EDC and Herceptin were run in the same manner as the reaction mixture.

General Characterizations. The surface morphology of Tam−PVP−PLGA NPs with and without herceptin antibody conjugation was examined by TEM (Tecnai G2 200 kV TEM (FEI)). The samples were prepared as reported by Vivek et al.[32] The average size and the surface charge (ζ potential) of the NPs were determined by DLS

technique and Zeta sizer (Malvern) instrumentation, respectively. The FT-IR spectra of NPs in the scan range of 500−4000 cm^{-1} were recorded using FT-IR spectrophotometer (Jasco, Japan). ^{1}H NMR spectroscopy was used to evaluate the conjugation of herceptin to the Tam−PVP−PLGA NPs.

Determination of Drug Loading and Encapsulation Efficiency. Studies on determination of drug loading (DL) and encapsulation efficiency (EE) of NPs were performed as reported elsewhere.[41] Briefly, 2 mg of freeze-dried Tam-PVP encapsulated PLGA NPs were dissolved in 200 μL of 1% acetic acid and vortexed. The solubilized Tam was quantified by HPLC using a fluorescence detector (Waters, Milford, U.S.A.). Tam fluorescence was detected at excitation/emission wavelengths of 260/339 nm. DL and EE were calculated using the following formulas:

$$DL\ (\%) = amount\ of\ drug\ in\ NPs/amount\ of\ NPs$$
$$quantified \times 100$$

$$EE\ (\%) = amount\ of\ drug\ in\ NPs/initial\ amount\ of\ drug \times 100$$

To quantify the amount of encapsulated Tam from PLGA particles, 2 mg of NPs was dissolved in 1 mL of 0.5 N NaOH solution and complete dissolution of NPs was determined by measuring the absorbance at 450 nm against a control NaOH solution.

In Vitro Drug Release Kinetics. To study the effect of HER2 antibody conjugation on drug release from the synthesized PVP−PLGA NPs, in vitro drug release from both Tam−PVP−PLGA NPs and herceptin−Tam−PVP−PLGA NPs was measured in triplicates. The release profiles of Tam from Tam loaded NPs at pH 7.4, 6.0, and 5.0 were studied using dialysis tube (MWCO ≈ 12−14 kDa) as reported elsewhere.[30,46] Samples were drawn at regular time intervals, and the Tam concentration was determined by HPLC as described earlier.[30]

Analysis of Cellular Uptake of NPs by Fluorescence Microscopy. The MCF-7 cells were grown in 6 well plates in a glass slides at the density of 5 × 10^4 cells/well and incubated for 24 h prior to adding 1 mL of coumarin-6 loaded PVP−PLGA NPs and herceptin−PVP−PLGA NPs at a concentration of 25 μg/mL. After incubation for 4 h, cells were washed thrice with ice cold PBS, fixed with 4% paraformaldehyde in PBS and visualized using Nikon Eclipse 80i fluorescence microscope (Nikon Instruments Inc., Japan).

Cellular Uptake Efficiency of NPs. The MCF-7 (5 × 10^4) cells were seeded in 96-well microtiter plate containing medium and grown for 24 h to reach required confluence. Then they were incubated with Tam−PVP−PLGA NPs and herceptin−Tam−PVP−PLGA NPs at 5 μg/mL concentration for 0.5, 1, 1.5, and 2 h, at 37 °C. A set of six wells was seeded with positive control and another with test samples. The sample wells were washed thrice with 50 mL of cold PBS and then added with 100 mL medium at regular intervals. Subsequently, the cells were lysed by treating with 50 mL of 0.5% Triton X100 in 0.2 N NaOH and the amount of Tam in cell lysates was determined using a fluorescence spectrometer (Shimadzu, Japan) with excitation and emission wavelengths of 254 and 380 nm, respectively. The cellular uptake efficiency was expressed as the percentage of fluorescence associated with the cells vs. the positive control solution.

Internalization of NPs in MCF-7 Cells by TEM. The ultrathin sections of cells were examined for distribution of NPs by TEM as reported by Vivek et al.[32] Briefly, MCF-7 cells were treated with NPs as stated earlier followed by wash with phosphate buffer to remove unbound NPs. The cells were then fixed, dehydrated in increasing concentration of acetone, and treated with spurr's low viscosity resin (Sigma-Aldrich, U.S.A.) in gradients. Acetone and spurr's low viscosity resin were used in the 3:1, 1:1 and 1:3 ratios. The sections of 60 nm thickness were stained with 0.5% uranyl acetate and analyzed by TEM.

In Vitro Cytotoxicity Study. The in vitro cytotoxicity of Tam, Tam−PVP−PLGA NPs, and herceptin−Tam−PVP−PLGA NPs were determined by MTT assay as reported elsewhere.[32,42] Briefly, the MCF-7 (1 × 10^4) cells were seeded onto 96-well plates and allowed to attach overnight in the culture medium. Then the medium in each well was carefully replaced with 100 μL of medium containing serially
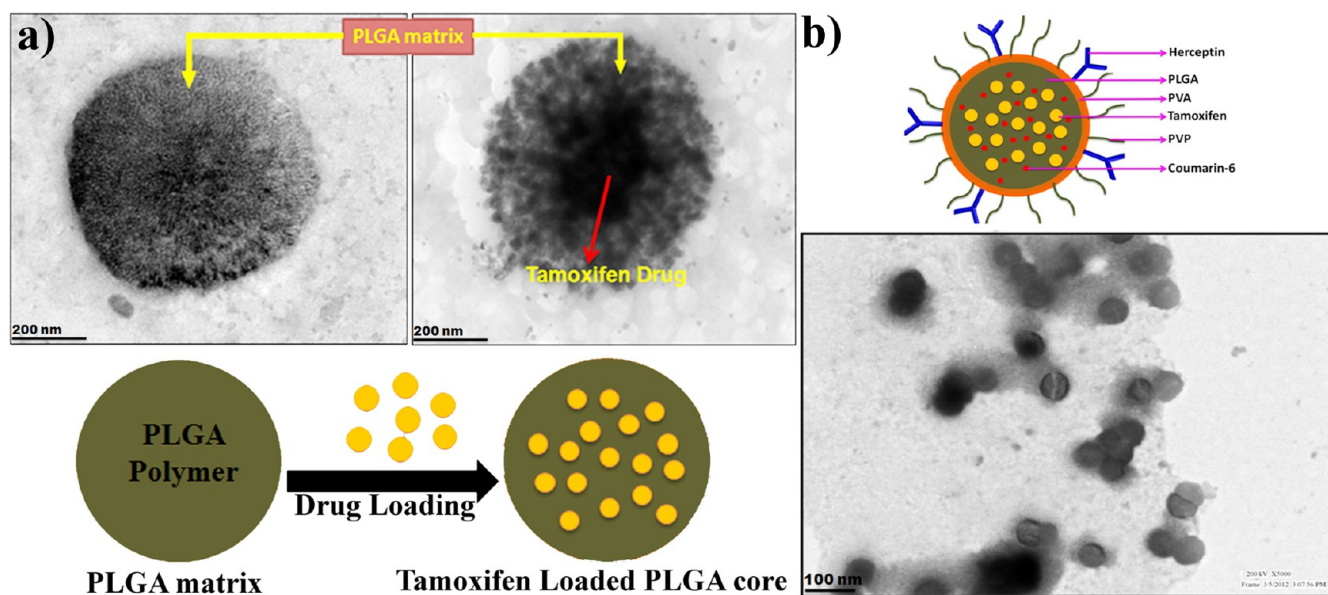
6471

dx.doi.org/10.1021/am406012g | ACS Appl. Mater. Interfaces 2014, 6, 6469−6480

Figure 1. (a) Representative TEM images of the synthesized PLGA–Tam drug core nanoparticles. (b) TEM image of herceptin-conjugated Tam-loaded PVP–PLGA.

diluted samples; the concentration of Tam used in each group was 1, 2, 4, 8, 16, and 32 μg/mL with the exposure duration of 48 h. At regular time intervals, 100 μL of MTT (5 mg/mL in PBS) was added to the wells and the cell viability assay was carried out by measuring the absorbance of wells at 620 nm using an ELISA plate reader. Experiments were carried out with seven parallel samples.

DAPI Staining. The MCF-7 cells (1×10^5 cells/coverslip) were incubated with NPs at their IC_{50} concentration, fixed in methanol: acetic acid (3:1 v/v) and stained with 5 μg/mL of DAPI for 20 min, and analysed for morphological changes using fluorescence microscope with excitation filter at 510–590 nm.

Flow Cytometry Analysis. For the detection of apoptosis in cancer cells, the cells were stained with Annexin V-FITC and propidium iodide (PI). In brief, the cells were pretreated with Tam, Tam–PVP–PLGA NPs, and herceptin–Tam–PVP–PLGA NPs at IC_{50} concentrations. The treated cells were suspended in 200 μL of binding buffer, and the suspension was added with 10 μL of Annexin V-FITC and 5 μL of PI followed by incubation for 15 min in dark at RT. Subsequently, 300 μL of binding buffer was added to the cell suspension and the cells were analyzed by a flow cytometer (BD, FACS Calibur, U.S.A.).

Western Blot Analysis. The MCF-7 cells were treated with free drug and drug loaded NPs at IC_{50} concentration for the induction of apoptosis. Subsequently, Western blot analysis was performed for cell extracts after determining their protein content by Bradford assay.[43] Fifty microgram protein samples were resolved by 12% SDS-polyacrylamide gel electrophoresis and then transferred to nitrocellulose membrane (Pall Corporation, U.S.A.). The membranes were immersed in blocking buffer (5% skim milk in PBS) for 1 h at RT and incubated overnight with primary antibodies such as survivin, Bcl-2, caspase 3, and β-actin. Immuno-reactivity was detected using the chemiluminescence system.

Assessment of Anti-tumor Activity. The anti-tumor efficiency of Tam-loaded NPs was assessed in tumor-induced mice as reported elsewhere.[44] Briefly, the subcutaneous dorsa of BALB/c nude mice were inoculated with MCF-7 cells (1×10^7) in 100 μL of normal saline. When the average volume of the xeno-graft tumor reached 70 mm^3, the mice were randomly divided into four groups with six mice in each group: group A, normal saline; group B, free Tam; group C, Tam–PVP–PLGA NPs; group D, herceptin–Tam-loaded PVP–PLGA NPs. Various Tam formulations with the drug concentration of 5 mg/kg was injected intravenously every 2 days, and the mice were then observed for 18 days.[44] The tumor diameters were measured

every 3 days interval for each group and the tumor volume (V) was calculated using the formula $V = [\text{length} \times (\text{width})^2]/2$. The sections of tumor, liver, and kidney tissues were stained with hematoxylin and eosin (HE) and the effects of NPs on these organs were studied.

Data Analysis. All the measurements were made in triplicates and the values were expressed as mean ± standard error of the mean. The results were subjected to Student t- test analysis and the data were considered statistically significant if $p < 0.05$.

■ RESULTS AND DISCUSSION

Characterization of Formulated NPs. PLGA polymer matrix stabilized with hydrated PVA (water phase) and Tam-loaded PLGA NPs with high drug payload were prepared and the morphological features were examined by TEM as shown in Figure 1a. Spherical nature of herceptin-conjugated Tam–PVP–PLGA polymer NPs is shown in Figure 1b. It was observed that the PVA was well coated in the polymeric NPs because of the hydrophobic interaction of PLGA. Because of the presence of amphiphilic PVA, the prepared NPs were well suspended in the aqueous phase. The synthesis of herceptin–Tam–PVP–PLGA NPs is favored by EDC via the formation of amide bond between the primary amine group of herceptin with the free carboxylic end group of Tam–PVP–PLGA NPs. Herceptin antibody could bind to the hydrophobic surface of PVP–PLGA through its constant region (F_c), leaving the antigen-binding sites (F_{ab}) free to interact with the antigen.[40] The conjugate and unconjugated structures were analyzed and confirmed by FT-IR and ^{1}H NMR spectroscopy of Tam–PVP–PLGA NPs (Figure S1, Supporting Information). Using FT-IR spectrum, the conjugation was quantitatively assessed by several characteristic vibrational modes (inset Figure of Figure S1b, Supporting Information). More specifically, the bands at ~1535 and 1627 cm^{-1} were assigned to C–O–C ether stretching vibration of NH$_2$–PVP–NH$_2$ and –COO stretching vibration of PLGA, respectively. The absorption band at 1573 cm^{-1} was attributed to phenyl ring in herceptin. ^{1}H NMR studies revealed peaks correspond to the benzene moiety of herceptin [δ = 7.311, 7.277, 7.242 ppm], PVP moiety [δ = 2.680, 2.337 ppm], and PLGA moiety [δ = 5.43–3.41 ppm]. DLS was used to determine the average hydrodynamic
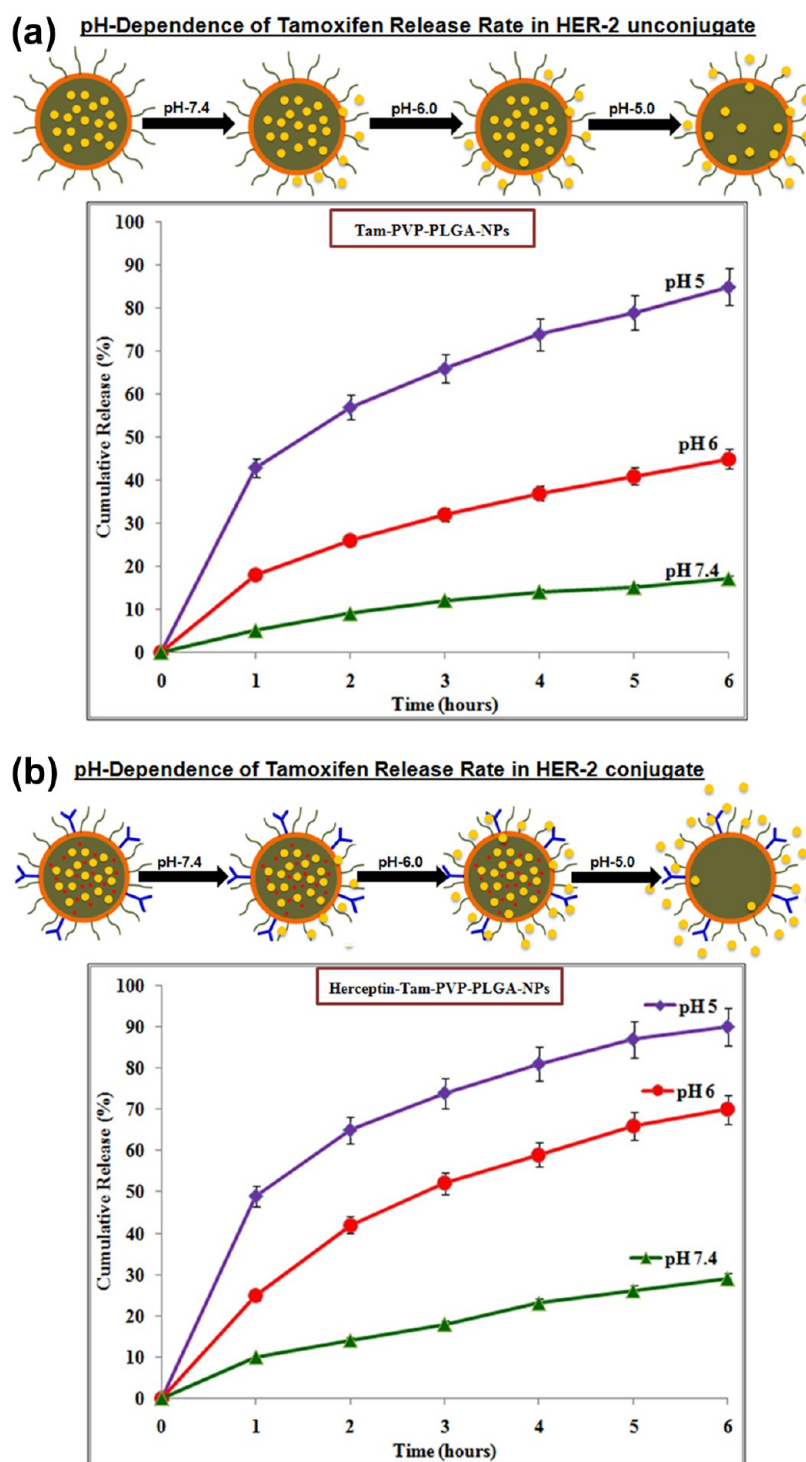
Figure 2. (a) pH-dependent in vitro drug release profiles from Tam−PVP−PLGA NPs at neutral (pH 7.4) and acidic (pH 6.0 and 5.0) conditions at 37 °C. Each point represents the mean ± SD. Error bars are based on triplicate measurements. (b) pH dependent in vitro drug release profiles from herceptin−Tam−PVP−PLGA NPs at neutral (pH 7.4) and acidic (pH 6.0 and 5.0) conditions at 37 °C. Each point represents the mean ± SD. Error bars are based on triplicate measurements.

diameters of particles and it was observed that there was an increase of ∼8 nm in the hydrodynamic diameter of Tam−PVP−PLGA NPs after addition of herceptin because of the presence of PLGA matrix. The sizes of Tam−PVP-PLGA NPs and herceptin-Tam loaded PVP−PLGA NPs were found to be 73.02 and 93.44 nm, respectively (Figure S2, Supporting Information). Because of herceptin conjugation, there was an increase in the size of herceptin-conjugated particles when

compared to unconjugated NPs. It was shown that the amount of herceptin covalently bound to the NP surface was ∼20 μg of herceptin per mg of NPs. It was reported that the size of NPs was appropriate for the penetration through the vascular system at tumor region to achieve passive targeting.[28,29] DLS data of the study revealed Herceptin dependent increase in the average size of the conjugated NPs, although high poly dispersity indexes (PDI) suggested the presence of heterogeneous
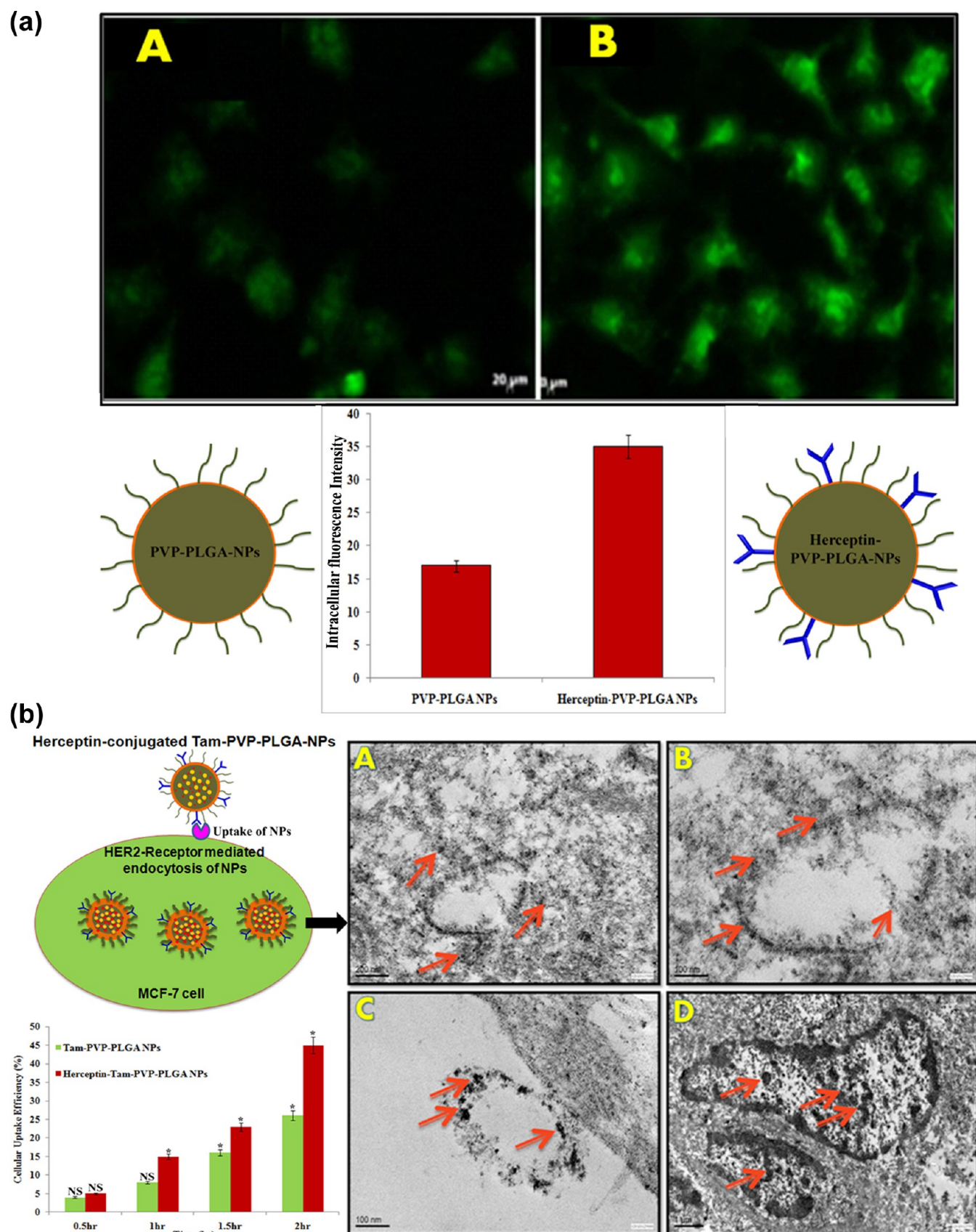
(a)

(b)

Figure 3. (a) Cellular uptake images of MFC-7 cells incubated with coumarin-6 with or without Herceptin conjugated NPs. Uptake of coumarin-6 loaded NPs is indicted by green fluorescence. (A) PVP–PLGA nanoparticles and (B) herceptin–Tam–PVP–PLGA nanoparticles. (b) Time-dependent cellular uptake efficiency of herceptin conjugated and unconjugated Tam–PVP–PLGA nanoparticles by MFC-7 cells after 0.5, 1, 1.5, and 2 h of incubation, respectively. Data represent mean ± SD. *$p < 0.05$ is considered statistically significant and [NS]not significant. TEM images of MFC-7 cell sections after (A) 0.5, (B) 1, (C) 1.5, and (D) 2 h of incubation with herceptin–Tam–PVP–PLGA NPs.

population of particles. DLS method was reliable in determining the overall size distribution of the particles and the PDI values for Tam−PVP−PLGA NPs and herceptin-Tam loaded PVP−PLGA NPs were found to be 0.455 and 0.272, respectively. The data on precise scattering properties of PLGA NPs in solution are also presented in Figure S2, Supporting Information. Though addition of PVP linker increased the size of NPs and it maintained a similar ζ potential because of the negative charge of the terminal carboxyl groups. Stability of the NPs could be due to reduction in cohesion between particles, which was revealed by high surface zeta potential values.[44] Tam−PVP−PLGA NPs exhibited negative charge with an average value of −35.24 ± 2.37 mV, whereas herceptin exhibited positive charge with a value of +8.4570.74 mV. This suggested that the Tam−PVP−PLGA NPs could be effectively coated with herceptin through electrostatic attraction between the two oppositely charged species. PVA is useful in forming stable NPs due to the display of slightly negative charged surface. The surface charge of the herceptin−Tam−PVP−PLGA NPs is −27.07 ± 1.68 mV (Figure S3, Supporting Information), which was similar to the data reported by Sun et al.[30] The preparation yield of Tam−PVP−PLGA NPs was found to be 83.5 ± 6.7%, and the encapsulation efficiency of Tam into PVP−PLGA NPs during loading of Tam in the concentration of 20 mg per 150 mg PLGA was 72.4 ± 2.3%.

pH-Dependent Tam Release. To test the influence of polymeric NPs on drug release, a study on Tam release profiles from NPs was performed in triplicates. The degradation of polymeric matrix allows the release of Tam from NPs. Furthermore, the duration and drug release levels from NPs will be modified by changing the formulation parameters such as drug-polymer ratio, and composition and molecular weight of the polymer.[31] To demonstrate the pH dependent drug release, Tam−PVP−PLGA NPs and herceptin−Tam loaded PVP−PLGA NPs were incubated in buffers at different pH and measured for Tam release at different time intervals. As shown in Figure 2a and 2b, release of Tam molecules was facilitated by the degradation of the polymer matrix. Tam release was slow and sustained at pH 7.4 with release rates of 17 ± 2.41% and 29 ± 0.27% in 6 h for Tam−PVP−PLGA NPs and herceptin−Tam−PVP−PLGA NPs, respectively. At pH 6.0, the release rates were found to be 45 ± 0.37% and 70 ± 2.28% for Tam−PVP−PLGA NPs and herceptin−Tam−PVP−PLGA NPs, respectively. However, at acidic pH 5.0, the rate of Tam release was much faster, and was found to be 85 ± 0.32% and 90 ± 2.11% for Tam−PVP−PLGA NPs and herceptin−Tam−PVP−PLGA NPs in 6 h, respectively. The results of in vitro drug release kinetics agree with the study by Sun et al. 2008,[30] wherein herceptin was reported to enhance drug release from the surface of PLGA NPs. Moreover, surface charge of PLGA NPs was positive at acidic pH, which reduced the electrostatic interaction of drug and PLGA NPs and thereby facilitated the drug release.[32] Hence, our findings substantiated the pH-dependent drug release behavior of the drug delivery system. It is plausible that much of the Tam-loaded NPs remain stable in the carrier at normal physiological pH 7.4 indicating the potential for prolonged drug retention time in blood circulation and thereby greatly reducing the adverse effects to normal tissues. On the other hand, the efficiency of cancer therapy is enhanced when these NPs are internalized by cancer cells via endocytosis followed by rapid Tam release from NPs inside the endosomes and lysosomes at acidic pH.[32,33] The release of Tam from nanocarrier at pH 5.0 resulted in increased fluorescence

intensity due to higher Tam release than at pH 6.0 and 7.0. Besides, the drug release from herceptin−Tam−PVP−PLGA NPs was significantly faster, that is, 90% than Tam−PVP−PLGA NPs at pH 5.0. The surface modification of HER2 antibody might facilitate drug diffusion from the polymeric matrix followed by the dissemination of drug to surrounding sites.

Nanoparticle Internalization. The present study showed that PLGA NPs, following the endocytosis-mediated cellular uptake, might undergo surface charge reversal in endolysosomes due to acidic pH prevailing in these organelles. This could facilitate an interaction of NPs with the endo-lysosome membranes, leading to transient and localized destabilization of the membranes and thereby resulting in the release of NPs into the cytosol.[34] However, the fraction of NPs that could escape the endosomal compartment might release the encapsulated Tam in a sustained manner due to slow degradation of polymer. It was also shown that Tam could be released from Tam−PVP−PLGA NPs from the acidic intracellular organelles during or after its accumulation in MCF-7 cells. We then investigated the entry mechanism of Tam−PVP−PLGA NPs into MCF-7 cells. Endocytosis is an important entry mechanism for various extracellular molecules, including the NPs of the present study. To evaluate the targeting ability of NPs, studies on cellular uptake of coumarin-6 loaded PVP−PLGA NPs and herceptin−PVP−PLGA NPs by MCF-7 cells were carried out. Fluorescence microscopy studies showed the distribution of coumarin-6 loaded NPs in the cytoplasm (Figure 3a), which indicated that the NPs were internalized by the cells. Besides, it was clearly shown that the intracellular fluorescence intensity of cells treated with HER2-targeted NPs was higher than that of the non-targeted NPs indicating the uptake of NPs by cells. The presence of Herceptin moiety on the outer surface of herceptin−PVP−PLGA NPs enabled the binding of NPs with HER2 receptors on breast cancer cells and subsequent receptor mediated endocytosis. The internalization of herceptin−PVP-PLGA NPs after 6 h of incubation was higher than coumarin-6 loaded PVP−PLGA NPs, resulting in stronger fluorescence intensity in MCF-7 cells. Intracellular fluorescence intensity for the group of herceptin−PVP−PLGA NPs produced 35 ± 2.6% enhancements compared to the group of PVP−PLGA NPs. The intensity of fluorescence from the liberated coumarin-6 was insignificant when compared to NPs internalized by cells.

These results substantiated that the synthesized herceptin−PVP−PLGA NPs could be an effective nanocarrier system for Tam delivery. These NPs also demonstrated significant properties in breast cancer therapy of HER2 overexpressed MCF-7 cells. The cellular uptake efficiency of the Tam−PVP−PLGA NPs was measured and compared with herceptin−Tam−PVP−PLGA NPs after 0.5, 1, 1.5, and 2 h in MCF-7 cell culture (Figure 3b). Cellular internalization of NPs was observed after incubation of cells with NPs. It can be seen from Figure 3b that the MCF-7 cells, after 0.5, 1, 1.5, and 2 h culture, exhibited enhanced uptake (*p <0.05) of herceptin−Tam−PVP−PLGA NPs when compared to herceptin unconjugated NPs. The cellular uptake efficiency of herceptin−Tam−PVP−PLGA NPs was found to be 5.1%, 15.3%, 23.6% and 45.2% at 0.5, 1, 1.5, and 2 h, respectively. Such results suggested that cellular uptake of NPs could be accelerated by Herceptin conjugated NPs. In clinical practice, HER2 has been considered as an essential indicator for breast cancer diagnosis, prognosis prediction, and development of therapeutic strategies. TEM

6475

dx.doi.org/10.1021/am406012g | ACS Appl. Mater. Interfaces 2014, 6, 6469−6480

images of MCF-7 cells treated with herceptin−Tam−PVP−PLGA NPs indicated the internalization of NPs by MCF-7 cells during different time intervals (0.5 to 2 h) (Figure 3b). It could be seen that herceptin−Tam−PVP−PLGA NPs exhibited higher cellular uptake efficiency than the NPs without Herceptin conjugation. Cell sections were observed by TEM to find out the intracellular distribution of NPs internalized by receptor-mediated endocytosis. TEM images showed well distributed NPs in the cytoplasm as well as in the nucleus of MCF-7 cells. It could be noted that cell and nuclear membranes appeared to be fragmented when internalization of Herceptin unconjugated NPs occurred. The results suggested that NPs entered into the cells via endocytosis process. Nanoparticle based DDS should have the features of target orientation, cell specificity, efficient cellular uptake of drug via endocytosis, subsequent localization into acidic organelles, and drug release.[32,34,35]

NP-Induced Enhanced Cytotoxicity in Targeted Cells. Herceptin-conjugated NPs could enhance the therapeutic efficacy of anticancer drugs because of their intrinsic toxicity to cancer cells and their ability in driving the nanocarriers to cytoplasm.[36,37,46,47] To demonstrate the cytotoxic effect of NPs, we carried out in vitro cytotoxicity study on MCF-7 cell line by MTT assay (Figure 4). At the end of 48 h exposure, we
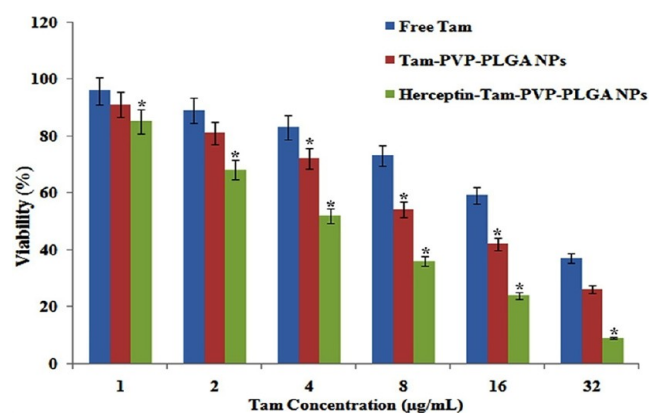

Figure 4. In vitro cytotoxic effect of MFC-7 cells after incubation with free Tam, Tam−PVP−PLGA NPs, and herceptin−Tam−PVP−PLGA NPs in concentration dependent cytotoxicity (IC_{50}) manner. Data represent mean ± SD. *$p < 0.05$ is considered statistically significant. Error bars are based on triplicate measurements.

observed that both free Tam and Tam-loaded PLGA NPs decreased the cell viability of MCF-7 cells. This suggests the use of PLGA NPs for enhancement of cytotoxicity effect of Tam on human breast cancer cells. In our case, the improvement in cytotoxicity of herceptin−Tam−PVP−PLGA NPs could be attributed to the higher uptake potential of the NPs by endocytosis mechanism when compared to Tam loaded NPs and free Tam. The cell viability (%) in the presence of Tam unloaded PLGA NPs and herceptin−PVP−PLGA NPs (100 μg/mL) was 99.8 ± 3.6% and 100 ± 1.2% suggesting that the NPs had no significant cytotoxicity effect on cells even at high doses. Tam-loaded NPs, Tam−PVP−PLGA NPs and herceptin−Tam−PVP−PLGA NPs with varied drug-loading levels and amounts were added to MCF-7 cells to evaluate their inhibition effect. Table 1 summarizes the IC_{50} values of nanoparticulate formulations and Tam free. IC_{50} values of Tam-loaded NPs (7.96 ± 0.41 μg/mL) and free Tam (13.21 ± 1.35 μg/mL) indicated that Tam-loaded NPs were more effective

Table 1. Evaluation of Cytotoxicity of Free Tamoxifen, Tam−PVP−PLGA NPs, and herceptin−Tam−PVP−PLGA NPs in MCF-7 Cells by MTT Assay

group	IC_{50} (μg/mL)
free tamoxifen	13.21 ± 1.35
Tam−PVP−PLGA NPs	7.96 ± 0.41
herceptin−Tam−PVP−PLGA NPs	3.24 ± 1.32

than free Tam in inhibiting cancer cell proliferation. The IC_{50} value for Herceptin conjugated NPs was found to be 3.24 ± 1.32 μg/mL (*p <0.05). The herceptin-conjugated NPs enhanced the cytotoxicity of Tam about 3.8 fold on MCF-7 cells when compared to free Tam treatment. Since the quantity of drug delivered into cells via NPs was high, the cells exhibited cytotoxic effect of the drug. After being treated with Tam of the equivalent concentration (16 μg/mL), the viability of MCF-7 cells treated with herceptin−PVP−PLGA NPs was lower (24.69%) than the cells treated with Tam-loaded PVP−PLGA NPs (41.58%). Targeted NPs exhibited better cytotoxic effects in MCF-7 cells than non-targeted NPs, and this could be due to the enhanced receptor-mediated internalization promoted by herceptin ligand.[44] Our earlier studies[32] reported that the Tam-loaded chitosan polymeric NPs had an enhanced cytotoxicity when compared to free Tam, and this was due to the rapid internalization and intracellular release of Tam from the polymer NPs. The cytotoxicity results suggested the therapeutic benefits of herceptin-conjugated polymeric NPs against HER2 overexpressed breast cancer cells.

Apoptosis of MCF-7 Cells. To study the mechanism of improvement in anticancer activity through apoptosis by pH based DDS, the nuclear DAPI staining was performed. By using the staining method, morphological changes of normal and apoptotic cells were studied. The untreated control MCF-7 cells showed normal nuclei whereas nanoparticle treated cells showed condensed or fragmented nuclei characteristic of apoptosis (Figure 5). Besides, nuclear morphological analysis revealed characteristic apoptotic features such as chromatin condensation, nuclear fragmentation, and apoptotic bodies in MCF-7 cells. To identify the induction of apoptosis by Tam-loaded NPs, flow cytometry analysis was performed wherein the fraction of apoptotic MCF-7 cells stained with Annexin V and PI was measured, following administration of Tam, Tam−PVP−PLGA NPs, and herceptin−Tam−PVP−PLGA NPs at IC_{50} concentration for 48 h. Cells in early apoptosis bind only to Annexin V, whereas dead and late stage apoptotic cells bind to both Annexin V and PI. Control group of MCF-7 cells showed negligible apoptotic, as well as necrotic activities (<5%). The percentage of early and late apoptotic cells was higher in the case of cells treated with Tam−PVP−PLGA NPs (74.58% and 8.64%) than the cells treated with unloaded PVP−PLGA NPs (16.02% and 1.4%) and free Tam (86.16% and 1.36%) (Figure 5). Treatment by all formulations showed negligible amount of necrotic cells, while control group of cells showed negligible apoptotic activity. Treatment by Tam−PVP−PLGA NPs caused a significant increase in programmed cell death, that is, 8.64% when compared to treatment by free Tam (1.36%) and unloaded PVP−PLGA NPs (1.4%), and this could be due to activation of apoptotic signaling pathway after internalization of NPs. Targeted delivery showed enhanced apoptosis of MCF-7 cells because of increase in receptor mediated endocytotic activity, resulting in high intracellular drug concentration available for induction of apoptosis.[45]
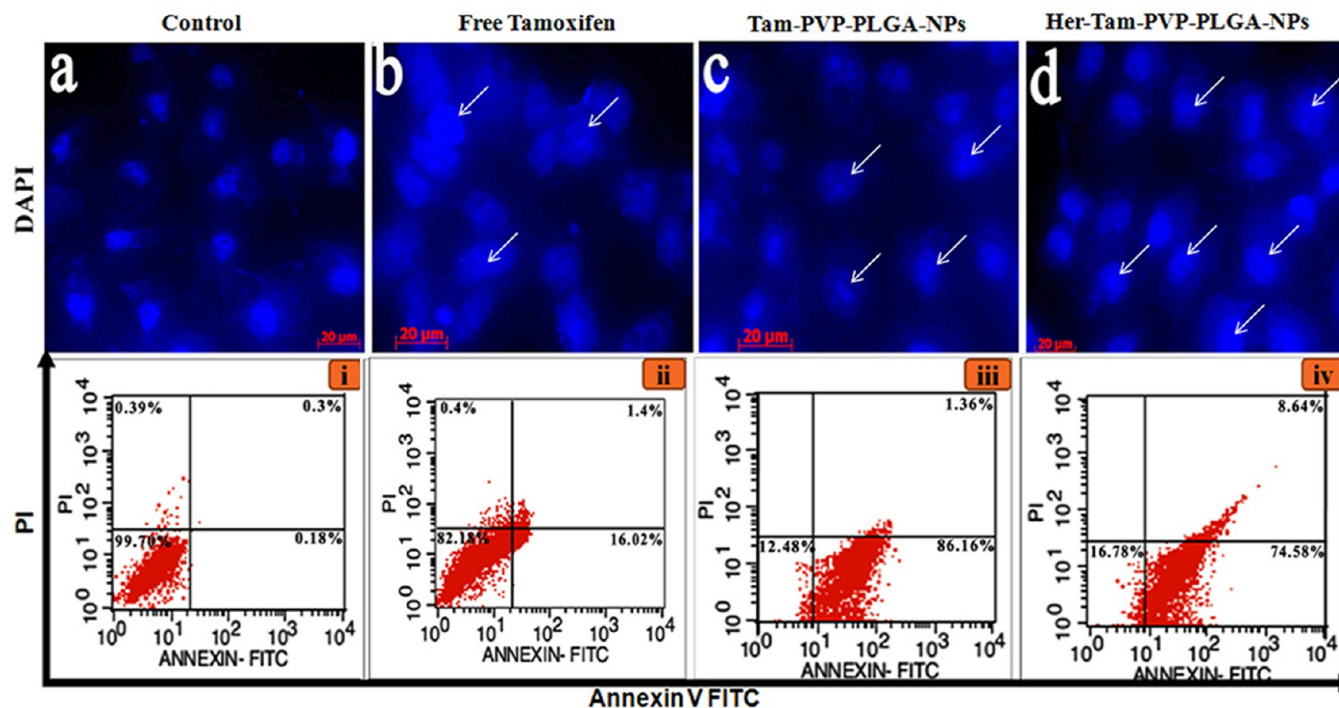
Figure 5. DAPI staining images of MCF-7 cells. The MCF-7 cells were treated with free Tam and Tam−PVP−PLGA NPs at IC$_{50}$ drug concentration for 48 h followed by visualization of DNA with DAPI staining using a fluorescence microscope. (a) Control, (b) Free Tam, (c) Tam−PVP−PLGA NPs, and (d) herceptin−Tam−PVP−PLGA NPs. The results are shown as a representative of four individual experiments ($n = 4$) (top panel). The cells were treated with free Tam, Tam−PVP−PLGA NPs, and herceptin−Tam−PVP−PLGA NPs at IC$_{50}$ drug concentration for 48 h and analyzed for apoptosis by flow cytometry. The fluorescence intensity of Annexin V + PI stained apoptotic cells is expressed as channel numbers in quadrant of plots; cells in bottom right and top right quadrants are in early and late apoptosis, respectively. The results are shown as a representative of four individual experiments ($n = 4$) (bottom panel).
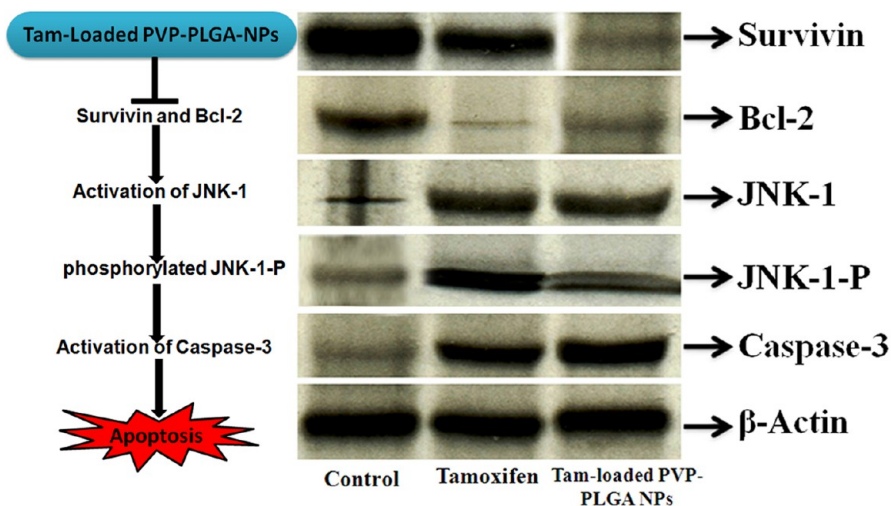

Figure 6. Up-regulation of JNK-1 signaling pathway in MFC-7 cells treated with Tam−PVP−PLGA NPs compared with Tam. The phosphorylation of JNK-1 by activation of caspase dependent apoptosis was analyzed by Western blotting.

Besides, slow and sustained cytoplasmic delivery of Tam from NPs could enhance the therapeutic efficiency of the NPs through apoptosis induction than the free Tam treatment. This suggested that the PVP modified PLGA NPs could serve as an effective drug delivery vehicles against breast cancer cells. Apoptotic signaling pathway is regulated by a complex network of molecules that alter the expression profiles of apoptotic proteins. Survivin is an important anti-apoptotic protein that arrests cell apoptosis via inhibiting the caspase activity. Caspase-3 is the critical factor for cell death, and is one of the major

activated caspases in apoptotic cells.[32] Consequently, we have performed Western blotting to confirm apoptosis of cells by analyzing the expression profiles of Survivin, Bcl-2, and Caspase proteins. Western blot analysis revealed the activation of JNK-1 signaling pathway with changes in the expression profiles of survivin, Bcl-2, and caspase proteins in MCF-7 cells treated with Tam when compared to Tam−PVP−PLGA NPs. We observed that the expression of survivin and Bcl-2 proteins were significantly down-regulated in cells cultured with Tam−PVP−PLGA NPs for 48 h (Figure 6). Inhibition of anti-apoptotic
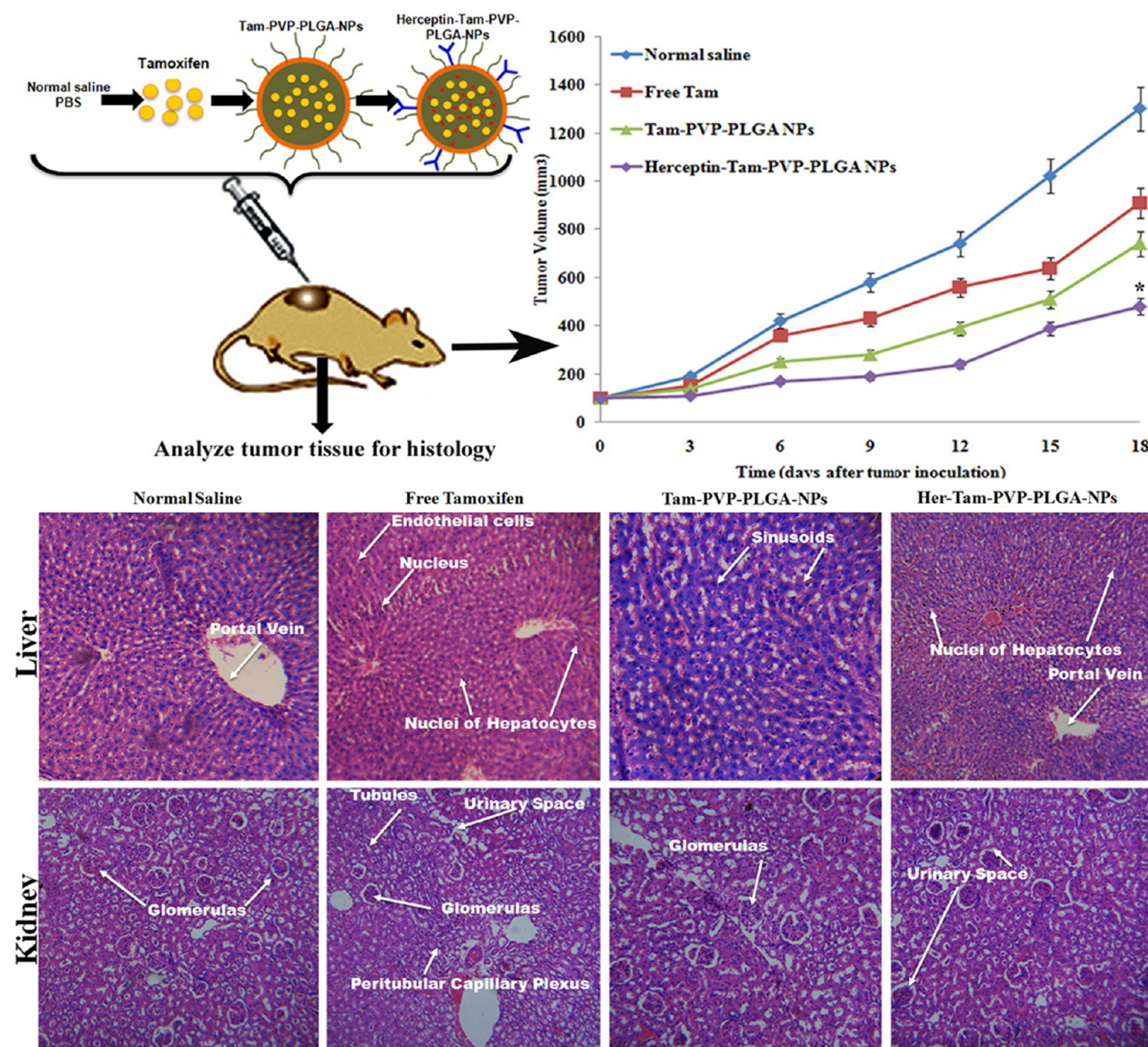
Figure 7. In vivo combination cancer therapy. Tumor growth curves of four different groups of mice after various treatments (4 mice/group) show varying degree of tumor suppression until the end of 18th day. The extent of tumor suppression is higher in herceptin–Tam–PVP–PLGA NPs treated group than others. Error bars are based on standard errors of the mean. *$p < 0.05$ was considered statistically significant. Images show HE stained sections of tumor slices collected after various treatments at the end of 18th day (scale bar = 50 μm).

functions of survivin and Bcl-2 and up-regulation of JNK-1 and caspase 3 prominently induced apoptosis in MCF-7 cells.

In Vivo Anti-tumor Activity. Normal saline, free Tam, Tam–PVP–PLGA NPs, and herceptin–Tam–PVP–PLGA NPs were injected at clinically relevant doses through the tail vein of the mice bearing breast carcinoma MCF-7 cells and the anti-tumor activity of NPs was assessed. Anti-tumor effect was more significant for the groups treated with free Tam and Tam-loaded NPs than the normal saline treated group (*$p < 0.05$). It was observed that the tumor volumes of NP-treated groups were smaller than the groups treated with free Tam and this could be due to sustained release behavior of Tam-loaded NPs and shorter half-life of Tam that was delivered without NPs. As depicted in Figure 7, the average tumor volume in herceptin-conjugated Tam-loaded NPs-treated mice group was gradually reduced to 478 mm³ at the end of 18 days after the final administration, while normal saline-treated mice group showed

no reduction in tumor volume (1311 mm³). The herceptin-conjugated-Tam-loaded NPs showed significantly higher anti-tumor activity than free Tam and Tam–PVP–PLGA NPs, with a mean tumor volume of 478.67 ± 135.21 (*$p < 0.05$). The inhibition rate of targeted NPs was higher (65.83%) than that the non-targeted NPs (49.51%). It is reported that the delivery of targeted NPs facilitates gradual accumulation of NPs in tumor tissue via receptor mediated endocytosis resulting in a potent anti-tumor activity.[38] However, non-conjugated NPs remain in extracellular matrix of the tumor tissue and undergo degradation or phagocytosis, resulting in release of the drug. The results are nearly similar as those reported elsewhere.[44] HE staining of the tissue sections was carried out to observe any change in the tissue following drug administration. The normal saline treated group showed characteristic tumor pathological features, that is, high quantity of enlarged cells with irregular shape, reduced cytoplasm, and deeply stained nuclei. The other

treatment groups showed a range of features of tumor necrosis, with fewer cancer cells having shrunken nuclei and more normal cells with increased cytoplasm when compared to normal saline group. However, the anti-tumor effects were prominently observed in the herceptin−Tam−PVP−PLGA NPs treated group by HE staining. Hence, it was clear that the targeted NPs could be well accumulated in the tumor tissue to exhibit action upon cancer cells. It is reported that the NPs accumulate in the liver following phagocytosis,[39] and liver toxicity is one of the adverse effects of Tam that limits its clinical application.[44] Staining of sections of liver in the free Tam group showed hydropic as well as fat degeneration, while there was no significant liver cell damage in the NPs treated groups except the minimal infiltration of inflammatory cells. The sections of kidneys of the mice treated with drug-loaded NPs showed normal glomerular structures, though minimal inflammatory cell infiltration was observed in the kidneys of free Tam-treated mice.

■ CONCLUSION

In this study, we developed herceptin-conjugated nanocarrier system for targeted delivery of Tam to improve the chemotherapy of HER2 overexpressed breast cancer cells. The formulated NPs were capable of sustained pH depended drug release. Herceptin−Tam−PVP-PLGA NPs demonstrated a superior cellular uptake, as well as cytotoxicity compared to Tam−PVP−PLGA NPs, and this is due to HER2 receptor mediated endocytosis of herceptin-conjugated NPs by breast cancer cells. Tam is then released from the NPs at acidic pH resulting in suppression of tumor cell growth through apoptosis. The results indicated that the formulated PVP−PLGA NPs were found to provide better anticancer and inhibitory activity against MCF-7 cells than free Tam, in vitro, and in vivo. Herceptin-conjugated Tam-loaded NPs showed remarkable enhancement in anticancer activity as shown by cytotoxicity studies, DAPI staining, and flow cytometry analysis. Besides, the possible JNK-1 mediated caspase-dependent apoptotic signalling pathway was confirmed by Western blot analysis. Using an in vivo mice model, significant tumor growth suppression was observed for the herceptin−PVP−PLGA NPs treated group. Furthermore, the conjugation of herceptin with PLGA NPs was an influential factor for tumor targeting. These results implied that NPs based DDS developed in this study could be effectively used for HER2-targeted MDR breast cancer therapy.

■ ASSOCIATED CONTENT

Ⓢ Supporting Information
[1]NMR study of tam-loaded PVP−PLGA NPs, ^{1}H NMR spectrum and FT-IR spectrum of herceptin-conjugated PVP−PLGA NPs, DLS examination of the particle size distribution with and without herceptin conjugation, ζ potential measurement analysis of nanoparticles with and without herceptin conjugation, tam−PVP−PLGA NPs, and herceptin−tam−PVP−PLGA NPs. This material is available free of charge via the Internet at http://pubs.acs.org/.

■ AUTHOR INFORMATION

Corresponding Authors
*E-mail: vivekproteomics@gmail.com.
*E-mail: skperiyaruniv@gmail.com; sk_protein@buc.edu.in.

Author Contributions
[⊥]R.V. and R.T. contributed equally.

■ REFERENCES

(1) Feng, S. S. Chemotherapeutic Engineering: Concept, Feasibility, Safety and Prospect—A Tribute to Shu Chien's 80th Birthday. *Cell. Mol. Bioeng.* **2011**, *4*, 708−716.

(2) Colotta, F. Anticancer Drug Discovery and Development. *Adv. Exp. Med. Biol.* **2008**, *610*, 19−42.

(3) Feng, S. S.; Chien, S. Chemotherapeutic Engineering: Application and Further Development of Chemical Engineering Principles for Chemotherapy of Cancer and other Diseases. *Chem. Eng. Sci.* **2003**, *58*, 4087−4114.

(4) Feng, S. S.; Zhao, L. Y.; Zhang, Z. P.; Bhakta, G.; Win, K. Y.; Dong, Y.C. Chemotherapeutic Engineering: Vitamin E TPGS-Emulsified Nanoparticles of Biodegradable Polymers Realized Sustainable Paclitaxel Chemotherapy for 168 h In Vivo. *Chem. Eng. Sci.* **2007**, *62*, 6641−6648.

(5) Petros, R. A.; DeSimone, J. M. Strategies in the Design of Nanoparticles for Therapeutic Applications. *Nat. Rev. Drug. Discovery* **2010**, *9*, 615−627.

(6) Jia, J.; Zhu, F.; Ma, X. H.; Cao, Z. W. W.; Li, Y. X. X.; Chen, Y. Z. Mechanisms of Drug Combinations: Interaction and Network Perspectives. *Nat. Rev. Drug. Discovery* **2009**, *8*, 111−128.

(7) Lehar, J.; Krueger, A. S.; Avery, W.; Heilbut, A. M.; Johansen, L. M.; Price, E. R. Synergistic Drug Combinations Tend to Improve Therapeutically Relevant Selectivity. *Nat. Biotechnol.* **2009**, *27*, 659−666.

(8) Woodcock, J.; Griffin, J. P.; Behrman, R. E. Development of Novel Combination Therapies. *New. Engl. J. Med.* **2011**, *364*, 985−997.

(9) Mitsiades, C. S.; Davies, F. E.; Laubach, J. P.; Joshua, D.; Miguel, J. S.; Anderson, K. C. Future Directions of Next-Generation Novel Therapies, Combination Approaches, and the Development of Personalized Medicine in Myeloma. *J. Clin. Oncol.* **2011**, *29*, 1916−1923.

(10) Mi, Y.; Liu, Y. T.; Guo, Y. J.; Feng, S. S. Herceptin (R)-Conjugated Nanocarriers for Targeted Imaging and Treatment of HER2-Positive Cancer. *Nanomedicine (London, U.K.)* **2011**, *6*, 311−322.

(11) Mi, Y.; Li, K.; Liu, Y.; Pu, K. Y.; Liu, B.; Feng, S. S. Herceptin Functionalized Polyhedral Oligomeric Silsesquioxanee Conjugated Oligomersesilica/Iron Oxide Nanoparticles for Tumor Cell Sorting and Detection. *Biomaterials* **2011**, *32*, 8226−8233.

(12) Esteva, F. J.; Valero, V.; Pusztai, L.; Boehnke-Michaud, L.; Buzdar, A. U.; Hortobagyi, G. N. Chemotherapy of Metastatic Breast Cancer: What to Expect in 2001 and Beyond. *Oncologist* **2001**, *6*, 133−146.

(13) Bullock, K.; Blackwell, K. Clinical Efficacy of Taxane-Trastuzumab Combination Regimens for HER-2-Positive Metastatic Breast Cancer. *Oncologist* **2008**, *13*, 515−525.

(14) Joensuu, H.; Lehtinen, P. K.; Bono, P.; Alanko, T.; Kataja, V.; Asola, R. Adjuvant Docetaxel or Vinorelbine with or without Trastuzumab for Breast Cancer. *New. Engl. J. Med.* **2006**, *354*, 809−820.

(15) Baselga, J.; Cortes, J.; Kim, S. B.; Im, S. A.; Hegg, R.; Im, Y. H. Pertuzumab Plus Trastuzumab Plus Docetaxel for Metastatic Breast Cancer. *N. Engl. J. Med.* **2012**, *366*, 109−119.

(16) Sullivan, S. P.; Murthy, N.; Prausnitz, M. R. Minimally Invasive Protein Delivery with Rapidly Dissolving Polymer Microneedles. *Adv. Mater. (Weinheim, Ger.)* **2008**, *20*, 933−938.

(17) Park, J. H.; Allen, M. G.; Prausnitz, M. R. Biodegradable Polymer Microneedles: Fabrication, Mechanics and Transdermal Drug Delivery. *J. Controlled Release* **2005**, *104*, 51−66.

(18) Aoyagi, S.; Izumi, H.; Fukuda, M. Biodegradable Polymer Needle with Various Tip Angles and Consideration on Insertion Mechanism of Mosquito's Proboscis. *Sens. Actuators, A* **2008**, *143*, 20−38.

(19) Kolli, C.S.; Banga, A. K. Characterization of Solid Maltose Micro Needles and their Use for Transdermal Delivery. *Pharm. Res.* **2008**, *25*, 104−113.

(20) Donnelly, R. F.; Majithiya, R.; Singh, T. R.; Morrow, D. I.; Garland, M. J.; Demir, Y. K. Design, Optimization and Characterisation of Polymeric Microneedle Arrays Prepared by a Novel Laser-based Micromoulding Technique. *Pharm. Res.* **2011**, *28*, 41−57.

(21) Matsumoto, A.; Matsukawa, Y.; Suzuki, T.; Yoshino, H. Drug Release Characteristics of Multi-Reservoir Type Microspheres with Poly (DL-lactide-*co*-glycolide) and poly(DL-lactide). *J. Controlled Release* **2005**, *106*, 172−180.

(22) Lee, J. W.; Park, J. H.; Prausnitz, M. R. Dissolving Microneedles for Transdermal Drug Delivery. *Biomaterials* **2008**, *29*, 2113−2124.

(23) Chu, L.Y.; Choi, S. O.; Prausnitz, M. R. Fabrication of Dissolving Polymer Microneedles for Controlled Drug Encapsulation and Delivery: Bubble and Pedestal Microneedle Designs. *J. Pharm. Sci.* **2010**, *99*, 4228−4238.

(24) Langer, R. Drug Delivery and Targeting. *Nature* **1998**, *392*, 5−10.

(25) Maeda, H.; Wu, J.; Sawa, T.; Matsumura, Y.; Hori, K. Tumor Vascular Permeability and the EPR Effect in Macromolecular Therapeutics: A Review. *J. Controlled Release* **2000**, *29*, 271−284.

(26) Fox, M. E.; Szoka, F. C.; Fréchet, J. M. Soluble Polymer Carriers for the Treatment of Cancer: The Importance of Molecular Architecture. *Acc. Chem. Res.* **2009**, *42*, 1141−1151.

(27) Duncan, R. The Dawning Era of Polymer Therapeutics. *Nat. Rev. Drug Discovery* **2003**, *2*, 347−360.

(28) Davis, M. E.; Chen, Z.; Shin, D. M. Nanoparticle Therapeutics: An Emerging Treatment Modality for Cancer. *Nat. Rev. Drug Discovery* **2008**, *7*, 771−782.

(29) Win, K. Y.; Feng, S. S. Effects of Particle Size and Surface Coating on Cellular Uptake of Polymeric Nanoparticles for Oral Delivery of Anticancer Drugs. *Biomaterials* **2005**, *26*, 2713−2722.

(30) Sun, B.; Ranganathan, B.; Feng, S. Multifunctional Poly(D,L-lactide-*co*-glycolide)/Montmorillonite (PLGA/MMT) Nanoparticles Decorated by Trastuzumab for Targeted Chemotherapy of Breast Cancer. *Biomaterials* **2008**, *29*, 475−486.

(31) Prabha, S.; Labhasetwar, V. Critical Determinants in PLGA/PLA Nanoparticle Mediated Gene Expression. *Pharm. Res.* **2004**, *21*, 354−364.

(32) Vivek, R.; Nipun Babu, V.; Thangam, R.; Subramanian, K. S.; Kannan, S. pH-Responsive Drug Delivery of Chitosan Nanoparticles as Tamoxifen Carriers for Effective Anti-Tumor Activity in Breast Cancer. *Cells Colloids Surf., B* **2013**, *111*, 117−123.

(33) Wang, F.; Wang, Y. C.; Dou, S.; Xiong, M. H.; Sun, T. M.; Wang, J. Doxorubicin-Tethered Responsive Gold Nanoparticles Facilitate Intracellular Drug Delivery for Overcoming Multidrug Resistance in Cancer. *Cells ACS Nano* **2011**, *5*, 3679−3692.

(34) Panyam, J.; Zhou, W. Z.; Prabha, S.; Sahoo, S. K.; Labhasetwar, V. Rapid Endo-Lysosomal Escape of Poly(DL-lactide-*co*-glycolide) Nanoparticles: Implications for Drug and Gene Delivery. *FASEB J.* **2002**, *16*, 1217−1226.

(35) Hu, X.; Tian, J.; Liu, T.; Zhang, G.; Liu, S. Photo-Triggered Release of Caged Camptothecin Prodrug from Dually Responsive Shell Cross-Linked Micelles. *Macromolecules* **2013**, *46*, 6243−6256.

(36) Zhao, J.; Mi, Y.; Liu, Y. T.; Feng, S. S. Quantitative Control of Targeting Effect of Anticancer Drugs Formulated by Ligand-Conjugated Nanoparticles of Biodegradable Copolymer Blend. *Biomaterials* **2012**, *33*, 1948−1958.

(37) Mi, Y.; Liu, X. L.; Zhao, J.; Ding, J.; Feng, S. S. Multimodality Treatment of Cancer with Herceptin Conjugated, Thermomagnetic Iron Oxides and Docetaxel Loaded Nanoparticles of Biodegradable Polymers. *Biomaterials* **2012**, *33*, 7519−7529.

(38) Jin, C.; Qian, N.; Zhao, W.; Yang, W.; Bai, L.; Wu, H.; Wang, M.; Song, W.; Dou, K. Improved Therapeutic Effect of DOX-PLGA-PEG Micelles Decorated with Bivalent Fragment HAb18 F(ab′) (2) for Hepatocellular Carcinoma. *Biomacromolecules* **2010**, *11*, 2422−2431.

(39) Avgoustakis, K.; Beletsi, A.; Panagi, Z.; Klepetsanis, P.; Livaniou, E.; Evangelatos, G.; Ithakissios, D. S. Effect of Copolymer Composition on the Physicochemical Characteristics, In Vitro Stability, and Biodistribution of PLGA−mPEG Nanoparticles. *Int. J. Pharm. (Amsterdam, Neth.)* **2003**, *259*, 115−127.

(40) Kocbek, P.; Obermajer, N.; Cegnar, M.; Kos, J.; Kristl, J. Targeting Cancer Cells Using PLGA Nanoparticles Surface Modified with Monoclonal Antibody. *J. Controlled Release* **2007**, *120*, 18−26.

(41) Primard, C.; Poecheim, J.; Heuking, S.; Sublet, E.; Esmaeili, F.; Borchard, G. Multifunctional PLGA-Based Nanoparticles Encapsulating Simultaneously Hydrophilic Antigen and Hydrophobic Immuno-modulator for Mucosal Immunization. *Mol. Pharmaceutics* **2013**, *10*, 2996−3004.

(42) Mosmann, T. Rapid Colorimetric Assay for Cellular Growth and Survival: Application to Proliferation and Cytotoxicity Assays. *J. Immunol. Methods* **1983**, *65*, 55−63.

(43) Gulfam, M.; Kim, J.E.; Lee, J. M.; Ku, B.; Chung, B. H.; Chung, B. G. Anticancer Drug-Loaded Gliadin Nanoparticles Induce Apoptosis in Breast Cancer. *Cells Langmuir* **2012**, *28*, 8216−8223.

(44) Liang, C.; Yang, Y.; Ling, Y.; Huang, Y.; Li, T.; Li, X. Improved Therapeutic Effect of Folate-Decorated PLGA−PEG Nanoparticles for Endometrial Carcinoma. *Bioorg. Med. Chem.* **2011**, *19*, 4057−4066.

(45) Chaudhari, R.; Kumar, A. K.; Khandelwal, V. K. M; Ukawala, M.; Manjappa, A.S.; Mishra, A. K.; Monkkonen, J.; Murthy, R. S. R. Bone Metastasis Targeting: A Novel Approach to Reach Bone Using Zoledronate Anchored PLGA Nanoparticle as Carrier System Loaded with Docetaxel. *J. Controlled Release* **2012**, *158*, 470−478.

(46) Zhao, S.; Tan, S.; Guo, Y.; Huang, J.; Chu, M.; Liu, H.; Zhang, Z. pH-sensitive Docetaxel-Loaded TPGS-poly(β-amino ester) Co-polymer Nanoparticles for Overcoming Multidrug Resistance. *Biomacromolecules* **2013**, *14*, 2636−2646.

(47) Zhao, J.; Mi, Y.; Feng, S. S. Targeted Co-Delivery of Docetaxel and siPlk1 by Herceptin-Conjugated Vitamin E TPGS Based Immunomicelles. *Biomaterials* **2013**, *34*, 3411−3421.

6480

dx.doi.org/10.1021/am406012g | *ACS Appl. Mater. Interfaces* 2014, 6, 6469−6480